CHEMICAL COMPOSITIONS OF RV TAURI STARS AND RELATED OBJECTS

S. Sumangala Rao and Sunetra Giridhar

Indian Institute of Astrophysics, Bangalore, India

RESUMEN

Hemos emprendido un análisis de las abundancias químicas para una muestra de estrellas RV Tauri poco estudiadas, para mejorar nuestro entendimiento de la evolución estelar post-secuencia asintótica de las gigantes (post-AGB). Nuestro estudio se basa en espectros de alta resolución y en una malla de modelos atmosféricos. Encontramos indicaciones de un leve proceso-s para V820 Cen y IRAS 06165+3158. Por otra parte, SU Gem y BT Lac muestran los efectos de una ligera separación polvo-gas. Hemos reunido los datos existentes sobre las abundancias de objetos RV Tauri, y encontramos que una gran parte de ellos muestra efectos de separación polvo-gas. En nuestro estudio encontramos un pequeño grupo de estrellas RV Tauri galácticas con evidencia del proceso-s ligeramente aumentado. Dos de tres objetos con evidencia de proceso-s aumentado pertenecen a la clase C de objetos RV Tauri. Estos objetos, pobres en metales, son candidatos prometedores para el estudio del proceso-s en las estrellas RV Tauri.

ABSTRACT

We have undertaken a comprehensive abundance analysis for a sample of relatively unexplored RV Tauri and RV Tauri like stars to further our understanding of post-Asymptotic Giant Branch (post-AGB) evolution. From our study based on high resolution spectra and a grid of model atmospheres, we find indications of mild s-processing for V820 Cen and IRAS 06165+3158. On the other hand, SU Gem and BT Lac exhibit the effects of mild dust-gas winnowing. We have also compiled the existing abundance data on RV Tauri objects and find that a large fraction of them are afflicted by dust-gas winnowing and aided by the present work, we find a small group of two RV Tauris showing mild s-process enhancement in our Galaxy. With two out of three reported s-process enhanced objects belonging to RV Tauri spectroscopic class C, these intrinsically metal-poor objects appear to be promising candidates to analyse the possible s-processing in RV Tauri stars.

Key Words: stars: abundances — stars: AGB and post-AGB — stars: variables

1. INTRODUCTION

RV Tauri stars are pulsating variables located in the instability strip along with the Cepheids but at relatively lower luminosities. Their characteristic light curves show alternating deep and shallow minima with a formal period (time elapsed between two consecutive deep minima) of $30-150$ days. Photometrically, there are two types of RV Tauri stars, RVa and RVb (Kukarkin, Parenago, & Kholopov 1958): RVa stars show a quasi-constant brightness of mean light whereas RVb stars exhibit a longer term variation in mean brightness with a period of about $600-1500$ days. Waelkens & Waters (1993) proposed that the RVb phenomenon is caused by either the dust ejected by the star or obscuration by the circumstellar shell as the star moves in the binary orbit. Extended multicolor photometry of a large sample of RV Tauri stars by Pollard et al. (1996) showed further complexity, such as damping of the short term (pulsational) variations at long term minima for a few RV Tauri stars, which was attributed to an interaction with the previously ejected matter or with the companion during certain orbital phases, thereby affecting the pulsation. The absence of secular varia-

tions in RVa does not necessarily imply that they are single stars; in fact, RVa objects are known to have binary companions, e.g., AC Her (see van Winckel et al. 1998) and RU Cen (see Maas, van Winckel, & Waelkens 2002). From a comprehensive study of RV Tauri binaries, van Winckel et al. (1999); Maas et al. (2002) proposed that the RV Tauri photometric types do not arise from a physical difference like spectral energy distributions (SEDs) and chemical composition but mainly from the viewing angle onto the disk. In this scenario the RVa objects are thought to be the ones with low inclination while objects with high inclination such that the disk is seen edge-on would appear as RVbs.

Preston et al. (1963) classified RV Tauri variables spectroscopically into RVA, RVB and RVC. RVA have spectral type G-K and near light minimum show TiO bands of abnormal strength. RVB are relatively warm weak-lined objects of spectral type F and exhibit strong CN and CH bands at light minimum. RVCs have weak metal lines in their spectra and have high radial velocities (Joy 1952). The CN and CH bands are weaker or absent at all phases. They are genuinely metal-poor objects.

As suggested by Wallerstein (2002) and van Winckel (2003) in their reviews RV Tauri stars are post-AGB objects crossing the instability strip. With the detection of RV Tauri stars in the Large Magellanic Cloud (LMC) by Alcock et al. (1998), their location on the high luminosity end of the population II instability strip is confirmed. Using the known distance modulus of the LMC, an absolute magnitude of -4.5 was estimated for RV Tauri variables with fundamental periods (time elapsed between a deep and a shallow minima) of about 50 days using the calibrated P-L-C (period-luminosity-color) relation by Alcock et al. (1998) further supporting the above suggestion. The detection of IR fluxes (Jura 1986) and the high estimated luminosities (Alcock et al. 1998) support the idea that these stars are in the post-AGB phase evolving towards the blue in the Hertzsprung-Russell (H-R) diagram.

Studies of the chemical compositions of RV Tauri variables were undertaken initially in large part to glean information about their evolutionary status and in particular about the compositional changes wrought by internal nucleosynthesis and mixing processes (dredge-ups). However, a considerable fraction of them exhibited a very different abundance peculiarity—a systematic depletion of refractory elements. A strong signature of this phenomenon has been observed in post-AGB objects like HR 4049,

HD 52961, BD+39°4926, HD 44179 etc (see van Winckel 2003, for a review). Through their study of λ Bootis stars showing similar depletions, Venn & Lambert (1990) noted the resemblance of the observed abundance pattern with that of the interstellar gas in which the metals are depleted through fractionation in the interstellar grains. Bond (1991) suggested that the extreme metal deficiency of HR 4049 like objects could be caused by the selective removal of metals through grain formation. A semi-quantitative model to explain this phenomenon observed in λ Bootis stars and HR 4049 like objects was developed by Mathis & Lamers (1992). These authors proposed two scenarios: capture by the presently visible post-AGB star of the depleted gas from the binary companion, or rapid termination of a vigorous stellar wind in a single star so that grains are blown outwards (and hence lost) resulting in a photosphere devoid of these grain forming elements. Waters, Trams, & Waelkens (1992) proposed an alternative scenario based upon slow accretion from the circumstellar or circum-system disk. This scheme provides favourable conditions for this effect to operate without any restriction on the nature of the binary companion. More observational support of this hypothesis, such as large [Zn/Fe] for HD 52961 (van Winckel, Mathis, & Waelkens 1992) and strong correlation between stellar abundance for IW Car and depletions observed in the interstellar gas demonstrated by Giridhar, Rao, & Lambert (1994), resulted in further detections of RV Tauri and post-AGB objects showing this effect, commonly referred to as 'dust-gas winnowing' or 'dust-gas separation'. A summary of these detections can be found in recent papers like Rao, Giridhar, & Lambert 2012; van Winckel et al. 2012. The condensation temperature (T_C)[1] being an important parameter measuring the propensity of a given element into grain formation, the dependence of the observed abundance on T_C can be used to identify these objects. For brevity, hereinafter we would refer to the 'dust-gas winnowing effect' as DG effect.

Among RV Tauris, this effect is most prevalent in RVB objects while their cooler sibling RVA only show weak manifestations, possibly due to the dilution caused by their deep convective envelopes. The genuinely metal-poor RVCs are unaffected by the DG winnowing since their metal-poor environment is not conducive for grain formation (Giridhar, Lambert, & Gonzalez 2000).

---

[1] The condensation temperature T_C is the temperature at which half of a particular element in a gaseous environment condenses into dust grains.

TABLE 1

THE PROGRAM STARS

No.	IRAS	Other Names	Period (Days)	Var Type
1	06165+3158	$\cdots$	$\cdots$	$\cdots$
2	$\cdots$	V820 Cen, SAO 205326	150	RV Tauri
3	06108+2743	SU Gem, HD 42806	50	RV Tauri
4	22223+5556	BT Lac	41	RV Tauri
5	$\cdots$	TX Per	78	RV Tauri
6	19135+3937	$\cdots$	$\cdots$	$\cdots$
7	01427+4633	SAO 37487, BD+46°442	$\cdots$	$\cdots$
8	07008+1050	HD 52961, PS Gem	71	SRD*
9	$\cdots$	V453 Oph, BD-02°4354	81	RV Tauri

*SRDs are semi-regular variable giants and supergiants of spectral types F, G and K. Sometimes emission lines are seen in their spectra. They have pulsation periods in the range of $30-1100$ days with an amplitude of variation upto the 4th magnitude in their light curves.

In the present work we have enlarged the RV Tauri sample by studying six unexplored RV Tauri stars and IRAS[2] objects located in or near the RV Tauri box in the IRAS two color diagram. We also present a more recent abundance analysis for the RVC star V453 Oph and the extremely depleted star HD 52961, which exhibits RVb like phenomenon in its light curve.

2. SELECTION OF THE SAMPLE

Our sample (see Table 1) comprises mainly unexplored RV Tauri stars, objects having RV Tauri like IR colors. We have also studied the known RV Tauri object V453 Oph and the heavily depleted object HD 52961 for which we provide a contemporary analysis covering more elements. The IR fluxes of known RV Tauri stars have been investigated by Lloyd Evans (1985) and Raveendran (1989). Lloyd Evans (1999) reported that the RV Tauri stars fall in a well-defined region of the IRAS two-color diagram called the RV Tauri box. This box is defined from the observed properties of RV Tauri dusty shells such as the temperatures at the inner boundary of the dust shell (T_{O}) and the absorption coefficient (Q) which depends on the density and the temperature distribution of the dust as well as on the chemical composition and the physical properties (like size) of the dust grains. Raveendran (1989), from his study of 17 sample RV Tauri stars, found that T_{O} had a range between 400-600K and Q between 0.15 to 0.5.

The study of SEDs of six RV Tauri objects by De Ruyter et al. (2005) showed a large near IR excess but low line of sight extinction. This, coupled with energy balance considerations suggested that the likely distribution of the circumstellar dust is that of a dusty disk. Lloyd Evans (1999) suggested that RV Tauris are those stars with dusty disks which are currently located within the instability strip. Lloyd Evans (1999) hence proposed that this RV Tauri box in the IRAS $[12]-[25]$, $[25]-[60]$ diagram enclosed by the limits $[12]-[25]=1.0-1.5$ and $[25]-[60]=0.20-1.0$, when supplemented by large near IR flux, provides an alternative method of searching for RV Tauri stars among IRAS objects.

In fact, the photometric monitoring of IRAS sources following the above mentioned criteria did result in finding new samples of RV Tauri objects studied by Maas et al. (2002) and Mass, van Winckel, & Lloyd Evans (2005).

In Figure 1 we have plotted our program stars (those having IR colors) which have been numbered according to Table 1. In the figure we have also plotted RV Tauri stars with known spectroscopic classification. Most of our program stars with the exception of BT Lac are located in or around the RV Tauri box.

Although a fraction of known RV Tauri stars are found in the RV Tauri box, many well known RV Tauri stars do not conform to these limits and lie outside the box. Perhaps the limits of RV Tauri box needs upward revision in both axes. Nevertheless this box provides a starting point for identifying RV Tauri candidates among IRAS sources with no photometry. In what follows we will refer as "RV Tauri like" those objects with RV Tauri like colors in the IRAS two colour diagram without photometric confirmation.

_____
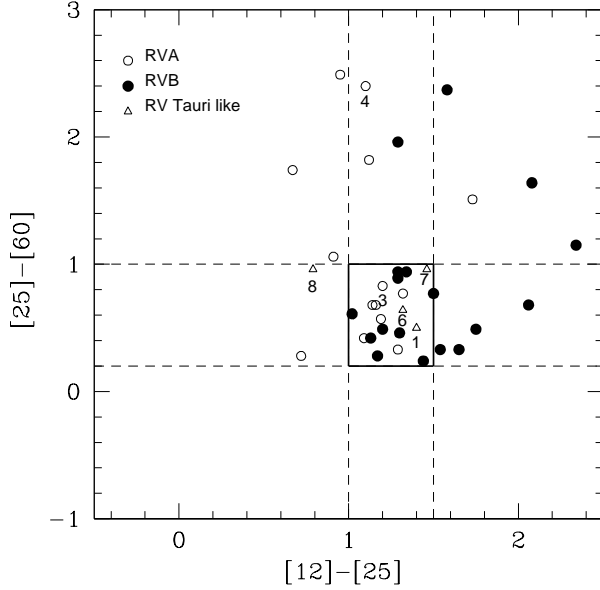[2]Infrared Astronomical Satellite.

Fig. 1. The IRAS color-color diagram showing the "RV Tauri" box. The figure contains our sample stars and all the well studied RV Tauri stars. The program stars are numbered according to Table 1.

Fig. 2. Sample spectra of our program stars presented in the descending order of temperature (top to bottom) in the 6100−6180 Å region.

3. OBSERVATIONS

High-resolution optical spectra were obtained at the W.J. McDonald Observatory with the 2.7 m Harlan J. Smith reflector and the Tull coudé spectrograph (Tull et al. 1995). This spectrometer gives a resolving power of about 60,000 and a broad spectral range was covered in a single exposure. A S/N ratio of 80−100 over much of the spectral range was achieved. Figure 2 illustrates the resolution and quality of sample spectra of our program stars in the wavelength region 6100−6180 Å. The sample spectra have been arranged in order of decreasing effective temperatures.

Program stars IRAS 06165+3158 and TX Per have the same effective temperature. The spectra of HD 52961 and V820 Cen were obtained with the echelle spectrometer of the 2.34 m Vainu Bappu Telescope at the Vainu Bappu Observatory (VBO) in Kavalur, India, giving a resolution of about 28,000 in the slitless mode (Rao et al. 2005).

4. ABUNDANCE ANALYSIS

The method of abundance analysis and the sources of log gf values have been described in detail by Rao et al. (2012), hereinafter Paper-1. The microturbulence velocity has been estimated by requiring that the derived abundances are independent of the line strengths. We have used Fe II lines
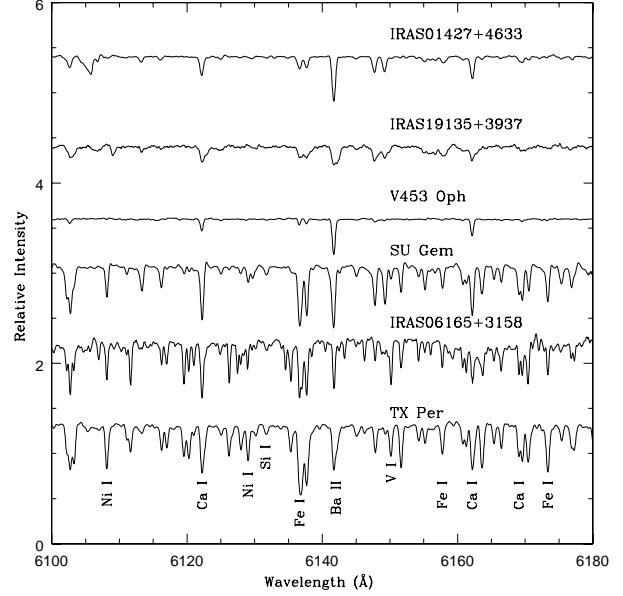
for warmer members but for cooler members, the paucity of usable Fe II lines compelled us to use Fe I lines. The temperatures have been determined by demanding that the iron abundance be independent of the lower excitation potential (LEP) and values for and log g have been determined from the excitation and ionization balance between Fe I and Fe II, Ti I and Ti II, Cr I and Cr II. We could not use hydrogen line profiles due to the presence of emission components and asymmetries present in most of the spectra. The derived stellar parameters are presented in Table 2. The sensitivity of the derived abundances to the uncertainties of atmospheric parameters $T_{\rm eff}$, log g and ξ is presented in Table 3. For three stars representing the full temperature range of our sample, we present changes in [X/Fe] caused by varying atmospheric parameters by 200 K, 0.25 cm s^{-2} and 0.5 km s^{-1} (average accuracies of these parameters) with respect to the chosen model for each star.

The abundances of elements for all our program stars are presented in Tables 4, 5, and 6 respectively.

The derived abundances relative to solar abundances are presented in these tables. The solar photospheric abundances given by Asplund, Grevesse, & Sauval (2005) have been used as reference. The possible systematic effects caused by the adopted gf values from different sources have been described in our Paper-1. For elements with lines exhibiting hy-

TABLE 2

STELLAR PARAMETERS DERIVED FROM THE FE-LINE ANALYSES

Star	UT Date	V_r[a] (km s^{-1})	T_{eff}, $\log g$, [Fe/H]	ξ_{t}[b] (km s^{-1})	Fe I[c] $\log \epsilon$	n	Fe II[c] $\log \epsilon$	n
IRAS 06165+3158	2007 Nov 5	−16.0	4250, 1.50, −0.93	2.8	6.54 ± 0.15	55	6.49 ± 0.17	6
V820 Cen	2011 Mar 02	+259.0	4750, 1.5, −2.28	2.4	5.14 ± 0.16	67	5.21 ± 0.15	8
V820 Cen	2011 Mar 03	+266.0	4750, 1.5, −2.35	2.4	5.06 ± 0.17	39	5.15 ± 0.01	2
IRAS 06108+2743	2009 Dec 26	+8.9	5250, 1.00, −0.25	3.0	7.20 ± 0.10	31	7.19 ± 0.10	14
IRAS 22223+5556	2009 Oct 10	−70.0	5000, 2.00, −0.17	3.7	7.28 ± 0.13	36	7.27 ± 0.14	4
TX Per	2009 Dec 27	−17.0	4250, 1.50, −0.58	3.1	6.81 ± 0.13	62	6.94 ± 0.13	7
IRAS 19135+3937	2007 Nov 3	−13.2	6000, 0.50, −1.04	4.1	6.46 ± 0.15	26	6.36 ± 0.09	7
IRAS 01427+4633	2007 Dec 21	−98.2	6500, 0.50, −0.79	3.5	6.71 ± 0.09	37	6.61 ± 0.11	8
HD 52961	2011 Jan 27	+4.2	6000, 0.5, −4.55	5.1	2.91 ± 0.00	1	2.89 ± 0.07	2
V453 Oph	2009 May 10	−125.9	5750, 1.50, −2.26	3.7	5.19 ± 0.10	28	5.18 ± 0.11	7

[a]V_r is the radial velocity in km s^{-1}.
[b]ξ_{t} is the microturbulence.
[c]$\log \epsilon$ is the mean abundance relative to H (with $\log \epsilon_{\mathrm{H}} = 12.00$). The standard deviations of the means as calculated from the line-to-line scatter are given. n is the number of considered lines.

TABLE 3

SENSITIVITY OF [X/FE] TO THE UNCERTAINTIES IN THE MODEL PARAMETERS FOR A RANGE OF TEMPERATURES COVERING OUR SAMPLE STARS

Species	TX Per (4250K) ΔT_{eff} −200K	$\Delta \log g$ +0.25	$\Delta \xi$ +0.5	IRAS 06108+2743 (5250K) ΔT_{eff} −200K	$\Delta \log g$ +0.25	$\Delta \xi$ +0.5	IRAS 01427+4633 (6500K) ΔT_{eff} −200K	$\Delta \log g$ +0.25	$\Delta \xi$ +0.5
C I	⋯	⋯	⋯	−0.29	−0.07	−0.09	−0.08	−0.01	−0.05
N I	⋯	⋯	⋯	⋯	⋯	⋯	−0.13	−0.06	−0.04
O I	+0.24	−0.01	−0.10	+0.03	−0.06	−0.09	⋯	⋯	⋯
Na I	+0.41	+0.22	−0.08	+0.05	+0.06	−0.07	⋯	⋯	⋯
Mg I	+0.25	+0.15	−0.02	+0.02	+0.06	−0.04	+0.03	+0.05	−0.01
Al I	+0.37	+0.19	−0.11	+0.03	+0.05	−0.10	+0.00	+0.06	−0.05
Si I	−0.05	+0.05	−0.08	+0.02	+0.05	−0.10	+0.00	+0.06	−0.06
Si II	⋯	⋯	⋯	⋯	⋯	⋯	−0.10	−0.07	+0.06
S I	⋯	⋯	⋯	+0.24	−0.06	−0.09	−0.05	+0.03	−0.06
Ca I	+0.48	+0.23	−0.01	+0.09	+0.06	−0.01	+0.04	+0.07	+0.00
Sc II	⋯	⋯	⋯	−0.02	−0.06	−0.01	−0.01	−0.05	−0.04
Ti I	⋯	⋯	⋯	−0.18	+0.07	−0.08	+0.07	+0.06	−0.03
Ti II	+0.13	+0.00	+0.02	−0.03	−0.06	+0.14	+0.13	−0.06	+0.14
Cr I	+0.43	+0.18	−0.08	+0.18	+0.07	+0.08	−0.05	+0.06	+0.05
Cr II	−0.09	−0.04	−0.06	−0.13	−0.07	−0.05	−0.07	−0.05	−0.01
Mn I	+0.37	+0.21	−0.05	+0.12	+0.07	+0.00	+0.02	+0.07	−0.06
Ni I	+0.19	+0.08	+0.01	+0.11	+0.06	+0.01	+0.03	+0.06	−0.04
Zn I	−0.04	+0.03	−0.01	+0.03	+0.01	+0.05	+0.02	+0.06	−0.05
Y II	⋯	⋯	⋯	−0.02	−0.06	+0.02	−0.02	−0.05	−0.05
Ce II	+0.24	−0.01	−0.10	+0.04	−0.05	−0.07	+0.04	−0.03	−0.05
Nd II	⋯	⋯	⋯	+0.05	−0.06	−0.10	⋯	⋯	⋯
Sm II	⋯	⋯	⋯	+0.04	−0.05	−0.08	⋯	⋯	⋯

perfine (hfs) and isotopic splitting, we have employed synthetic spectra in deriving abundances. For the elements Sc and Mn, we have used the hfs component list and their log *gf* given by Prochaska & McWilliam (2000), for Eu (Mucciarelli et al. 2008) and for Ba (McWilliam 1998).

TABLE 4

ELEMENTAL ABUNDANCES FOR IRAS 06165+3158 AND V820 CEN

Species	$\log \epsilon_\odot$	IRAS 06165+3158			V820 Cen[a]			V820 Cen[b]		
		[X/H]	N	[X/Fe]	[X/H]	N	[X/Fe]	[X/H]	N	[X/Fe]
O I	8.66	-0.49 ± 0.00	1	$+0.44$	-0.82 ± 0.00	1	$+1.46$	$\cdots$		
Na I	6.17	-0.47 ± 0.05	3	$+0.46$	-1.86 ± 0.00	1	$+0.42$	$\cdots$		
Mg I	7.53	-0.90 ± 0.06	2	$+0.03$	-1.95 ± 0.09	2	$+0.33$	-2.04 ± 0.00	1	$+0.31$
Mg II	7.53	$\cdots$			$\cdots$			-2.07 ± 0.00	1	$+0.28$
Si I	7.51	-0.86 ± 0.10	8	$+0.07$	-1.46 ± 0.11	4	$+0.82$	$\cdots$		
Ca I	6.31	-1.22 ± 0.13	11	-0.29	-1.95 ± 0.12	9	$+0.33$	-2.03 ± 0.15	5	$+0.32$
Sc II	3.05	-0.95 ± 0.02	1s*	-0.03	-1.78 ± 0.16	3	$+0.50$	-1.83 ± 0.00	1	$+0.52$
Ti I	4.90	-0.96 ± 0.12	15	-0.03	-1.77 ± 0.06	2	$+0.51$	-1.76 ± 0.12	10	$+0.59$
Ti II	4.90	-1.10 ± 0.14	6	-0.17	-1.90 ± 0.14	11	$+0.38$	-1.83 ± 0.13	3	$+0.52$
Cr I	5.64	-0.66 ± 0.08	8	$+0.27$	-2.50 ± 0.08	6	-0.22	-2.45 ± 0.11	4	-0.10
Cr II	5.64	-0.79 ± 0.00	1	$+0.14$	-2.40 ± 0.00	1	-0.12	$\cdots$		
Mn I	5.39	-1.22 ± 0.04	5	-0.29	-2.46 ± 0.01	2	-0.18	$\cdots$		
Fe	7.45	-0.93			-2.28			-2.35		
Ni I	6.23	-0.69 ± 0.06	6	$+0.24$	-2.21 ± 0.15	11	$+0.07$	-2.08 ± 0.08	2	$+0.27$
Zn I	4.60	-0.99 ± 0.01	2	-0.06	-1.84 ± 0.20	2	$+0.44$	$\cdots$		
Sr I	2.92	$\cdots$			-1.77 ± 0.00	1	$+0.51$	-1.71 ± 0.00	1	$+0.64$
Y II	2.21	-0.55 ± 0.04	2	$+0.38$	-2.07 ± 0.13	1s*	$+0.21$	-1.98 ± 0.15	2	$+0.37$
Zr I	2.59	-0.27 ± 0.07	5	$+0.66$	$\cdots$			$\cdots$		
Zr I	2.59	-0.27 ± 0.04	1s*	$+0.66$	$\cdots$			$\cdots$		
Zr II	2.58	$\cdots$			-1.80 ± 0.14	3	$+0.48$	-1.88 ± 0.00	1	$+0.47$
Ba II	2.17	$\cdots$			-1.74 ± 0.01	1s*	$+0.54$	$\cdots$		
La II	1.13	-0.67 ± 0.07	2	$+0.26$	-1.76 ± 0.17	2	$+0.52$	$\cdots$		
Ce II	1.58	-0.63 ± 0.14	4	$+0.30$	-1.93 ± 0.12	3s*	$+0.35$	-2.07 ± 0.05	2	$+0.28$
Pr II	0.78	-0.37 ± 0.00	1s*	$+0.56$	$\cdots$			$\cdots$		
Nd II	1.45	-0.63 ± 0.01	2	$+0.30$	-1.98 ± 0.18	4	$+0.30$	-2.17 ± 0.02	2	$+0.20$
Nd II	1.45	-0.73 ± 0.03	1s*	$+0.20$	$\cdots$			$\cdots$		
Sm II	1.01	-0.67 ± 0.11	3	$+0.26$	-1.85 ± 0.12	4	$+0.43$	-1.79 ± 0.01	2	$+0.56$

*The number of features synthesized for each element has been indicated.

[a]The abundance measurements of V820 Cen for March 2, 2011.

[b]The abundance measurements of V820 Cen for March 3, 2011.

5. RESULTS

There are several processes that affect the stellar composition during the course of its evolution such as (a) the initial composition of the interstellar medium (ISM), (b) the effect of nucleosynthesis and mixing processes such as dredge-ups, (c) DG winnowing that affects a large number of the studied RV Tauri stars and post-AGBs, (d) for a very small group of objects the abundances show dependencies on their first ionization potential (FIP). In the following subsections on individual stars, we discuss the derived abundances to infer the influence of these effects operating in our program stars.

5.1. New sample

5.1.1. IRAS 06165+3158

Miroshnichenko et al. (2007) gives the spectral type as K5Ib, remark that the star is 'probably metal

deficient', and describe a strong IRAS infrared excess due to cold dust. No OH maser emission at 1612 MHz was detected for this star (Lewis, Eder, & Terzian 1990). No photometric observations have been reported so the variable type and period are unknown. This star has been included in our analysis as it had RV Tauri like colors in the two-color diagram, as can be seen in Figure 1.

Our abundance analysis confirms that this star is metal-deficient ([Fe/H] = -0.93). Mild enrichment of s-process elements (Y, Zr, La, Ce, Nd and Sm) and also that of Pr, an r-process element is seen, with an average [s/Fe] of $+0.4$ dex (see Table 4). Due to the low temperature of the star and very poor S/N ratio in blue the number of clean s-process element lines (even for synthesis) is woefully small. The Ba II feature at 6141.7 Å has doubling in the core and the one at 5853.6 Å has a distinct unresolved compo-

TABLE 5

ELEMENTAL ABUNDANCES FOR IRAS 06108+2743, IRAS 22223+5556,
TX PER AND IRAS 19135+3937

Species	$\log \epsilon_\odot$	IRAS 06108+2743			IRAS 22223+5556			TX Per			IRAS 19135+3937		
		[X/H]	N	[X/Fe]	[X/H]	N	[X/Fe]	[X/H]	N	[X/Fe]	[X/H]	N	[X/Fe]
C I	8.39	−0.10 ± 0.01	1s*	+0.15	⋯			⋯			−0.23 ± 0.11	4	+0.81
O I	8.66	−0.02 ± 0.10	2	+0.23	+0.56 ± 0.00	1	+0.73	−0.11 ± 0.11	2	+0.47	−0.29 ± 0.00	1	+0.75
Na I	6.17	−0.06 ± 0.09	3	+0.19	+0.41 ± 0.01	2	+0.58	−0.68 ± 0.13	3	−0.10	−0.87 ± 0.00	1	+0.17
Mg I	7.53	−0.21 ± 0.02	2	+0.04	+0.02 ± 0.00	1	+0.19	−0.57 ± 0.08	2	+0.01	−0.75 ± 0.02	2	+0.29
Al I	6.37	−0.66 ± 0.08	4	−0.41	⋯			−0.80 ± 0.00	1	−0.22	⋯		
Si I	7.51	−0.28 ± 0.08	9	−0.03	−0.11 ± 0.17	5	+0.06	−0.19 ± 0.07	6	+0.39	⋯		
S I	7.14	+0.14 ± 0.00	1	+0.39	⋯			⋯			−0.74 ± 0.02	2	+0.30
Ca I	6.31	−0.67 ± 0.07	8	−0.42	−0.56 ± 0.07	3	−0.39	−1.12 ± 0.07	8	−0.54	−1.33 ± 0.17	4	−0.29
Ca II	6.31	⋯			⋯			⋯			−1.37 ± 0.00	1	−0.33
Sc II	3.05	−0.51 ± 0.04	4	−0.26	−0.53 ± 0.02	2	−0.36	⋯			−1.23 ± 0.01	3	−0.19
Ti I	4.90	−0.68 ± 0.05	4	−0.43	−0.57 ± 0.12	11	−0.40	−0.88 ± 0.09	9	−0.30	⋯		
Ti II	4.90	−0.57 ± 0.16	4	−0.32	−0.68 ± 0.01	2	−0.51	−0.79 ± 0.04	2	−0.21	−1.54 ± 0.10	4	−0.50
Cr I	5.64	−0.38 ± 0.10	4	−0.13	−0.14 ± 0.03	2	+0.03	−0.56 ± 0.05	4	+0.02	−1.20 ± 0.16	3	−0.16
Cr II	5.64	−0.36 ± 0.02	3	−0.11	−0.23 ± 0.00	1	−0.06	−0.66 ± 0.03	2	−0.08	−1.19 ± 0.13	7	−0.15
Mn I	5.39	−0.38 ± 0.04	3	−0.13	−0.40 ± 0.11	1s*	−0.23	−0.76 ± 0.12	6	−0.18	−1.05 ± 0.19	2	−0.01
Fe	7.45	−0.25			−0.17			−0.58			−1.04		
Ni I	6.23	−0.30 ± 0.17	6	−0.05	−0.22 ± 0.11	18	−0.05	−0.84 ± 0.10	10	−0.26	−0.86 ± 0.14	5	+0.18
Zn I	4.60	−0.16 ± 0.01	2	+0.09	−0.12 ± 0.05	2	+0.05	−0.86 ± 0.07	2	−0.28	−1.08 ± 0.01	2	−0.04
Y II	2.21	−0.69 ± 0.10	3	−0.44	−0.66 ± 0.09	2	−0.49	⋯			−1.33 ± 0.07	2	−0.29
Zr I	2.59	⋯			⋯			−1.40 ± 0.04	2	−0.82	⋯		
Zr II	2.59	⋯			−0.70 ± 0.00	1	−0.53	⋯			−1.17 ± 0.12	2	−0.13
La II	1.13	⋯			⋯			⋯			−1.85 ± 0.00	1	−0.81
Ce II	1.58	−0.84 ± 0.13	3	−0.59	−0.36 ± 0.05	3	−0.19	−1.35 ± 0.04	3	−0.77	−1.63 ± 0.00	1	−0.59
Nd II	1.45	−1.00 ± 0.07	3	−0.75	⋯			⋯			−1.28 ± 0.00	1	−0.24
Sm II	1.01	−0.66 ± 0.05	3	−0.41	−0.50 ± 0.12	2	−0.33	⋯			⋯		

*The number of features synthesized for each element has been indicated.

nent; hence it could not be used. The estimated s-process abundances are supported by the synthesis of these features as can be seen in Figure 3. The O abundance has been determined from the forbidden line at 6300.3 Å. But the C abundance is surprisingly low. The CH bands in the 4300 Å region, as well as the C_2 bands in the 5150−5165 Å region, appear weak, and synthesis indicates [C/H] < −2.0.

This is an atypical star in the sense that at a metallicity of −0.93, the expected enrichment of α elements is not seen ([Ca/Fe] = −0.3, [Ti/Fe] = [Si/Fe] = [Mg/Fe] = 0). Also the s-process enrichment is not accompanied by C-enrichment. A continuous photometric and spectrometric monitoring is required to detect the cause of s-process enhancement (binarity?).

5.1.2. V820 Cen

V820 Cen is listed as an RV Tauri variable in the General Catalogue of Variable Stars (GCVS) with a period of 150 days, but photometry (Eggen 1986; Pollard et al. 1996) shows considerable variations in the light curve, with Pollard et al. (1996) finding three main periods (148, 94 and 80 days). It is assigned a photometric type RVa and the spectroscopic type has not been given.
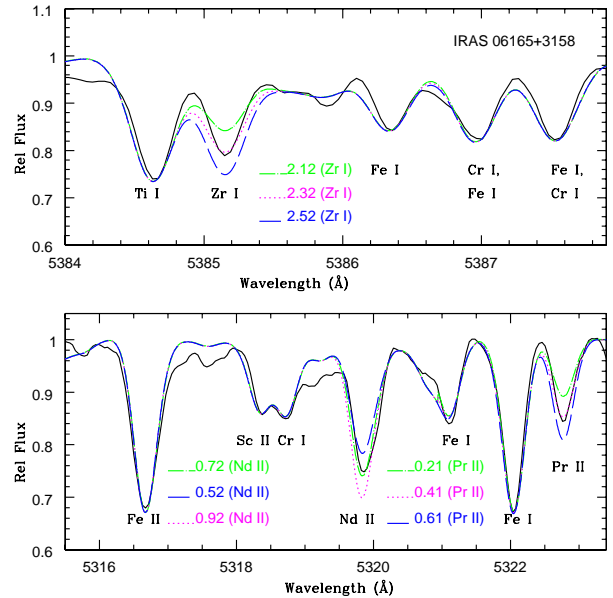

Fig. 3. The agreement between synthesized and observed spectrum for IRAS 06165+3158 for selected regions containing the lines of s-process elements.

TABLE 6

ELEMENTAL ABUNDANCES FOR IRAS 01427+4633, HD 52961 AND V453 OPH

Species	$\log \epsilon_\odot$	IRAS 01427+4633			HD 52961			V453 Oph		
		[X/H]	N	[X/Fe]	[X/H]	N	[X/Fe]	[X/H]	N	[X/Fe]
C I	8.39	-0.55 ± 0.11	5	$+0.24$	-0.15 ± 0.22	19	$+4.39$	-2.39 ± 0.01	CHs[†]	-0.13
N I	7.78	$+0.02 \pm 0.05$	3	$+0.81$	$+0.08 \pm 0.00$	1	$+4.62$	$\cdots$		
O I	8.66	-0.50 ± 0.01	3s*	$+0.29$	-0.38 ± 0.03	2	$+4.16$	-1.39 ± 0.00	1	$+0.87$
Na I	6.17	$\cdots$			-1.10 ± 0.01	2	$+3.44$	-1.91 ± 0.00	1	$+0.35$
Mg I	7.53	-0.50 ± 0.06	4	$+0.29$	-3.74 ± 0.02	2	$+0.80$	-1.95 ± 0.06	4	$+0.31$
Mg II	7.53	$\cdots$			-3.68 ± 0.00	1	$+0.86$	$\cdots$		
Al I	6.37	$\cdots$			$\cdots$			-2.68 ± 0.04	2	-0.44
Si I	7.51	-0.32 ± 0.09	3	$+0.47$	$\cdots$			-1.61 ± 0.06	2	$+0.65$
Si II	7.51	-0.38 ± 0.00	1	$+0.41$	-3.08 ± 0.00	1	$+1.46$	-1.72 ± 0.02	2	$+0.54$
S I	7.14	-0.42 ± 0.05	2	$+0.37$	-0.92 ± 0.11	4	$+3.62$	$\cdots$		
Ca I	6.31	-0.65 ± 0.04	5	$+0.14$	$\cdots$			-2.12 ± 0.04	4	$+0.14$
Ca II	6.31	$\cdots$			-3.61 ± 0.00	1	$+0.90$	$\cdots$		
Sc II	3.05	-0.41 ± 0.07	4	$+0.38$	$\cdots$			-2.10 ± 0.01	1s*	$+0.16$
Ti I	4.90	-0.31 ± 0.09	2	$+0.48$	$\cdots$			$\cdots$		
Ti II	4.90	-0.30 ± 0.02	2	$+0.49$	-4.27 ± 0.00	1	$+0.27$	-1.93 ± 0.11	10	$+0.33$
Cr I	5.64	-0.91 ± 0.12	2	-0.12	$\cdots$			-2.49 ± 0.08	4	-0.23
Cr II	5.64	-0.90 ± 0.11	6	-0.11	$\cdots$			-2.45 ± 0.07	2	-0.19
Mn I	5.39	-0.91 ± 0.07	2	-0.12	$\cdots$			-2.59 ± 0.00	1s*	-0.33
Fe	7.45	-0.79			-4.54			-2.26		
Ni I	6.23	-0.55 ± 0.12	5	$+0.24$	$\cdots$			-2.52 ± 0.10	4	-0.26
Zn I	4.60	-0.87 ± 0.07	2	-0.08	-1.27 ± 0.09	3	$+3.27$	-1.90 ± 0.11	2	$+0.36$
Sr II	2.92	$\cdots$			-4.33 ± 0.00	1	$+0.21$	$\cdots$		
Y II	2.21	-1.07 ± 0.00	1	-0.28	$\cdots$			-1.93 ± 0.06	4	$+0.33$
Zr II	2.59	$\cdots$			$\cdots$			-1.58 ± 0.11	4	$+0.68$
Ba II	2.17	-0.64 ± 0.02	1s*	$+0.15$	-4.26 ± 0.00	1	$+0.28$	-1.91 ± 0.08	2	$+0.35$
La II	1.13	$\cdots$			$\cdots$			-1.54 ± 0.00	2	$+0.72$
Ce II	1.58	-0.98 ± 0.14	3	-0.19	$\cdots$			-1.61 ± 0.08	4	$+0.65$
Nd II	1.45	$\cdots$			$\cdots$			-1.60 ± 0.12	4	$+0.66$
Eu II	0.52	$\cdots$			$\cdots$			-1.22 ± 0.00	1s*	$+1.04$
Gd II	1.14	$\cdots$			$\cdots$			-1.23 ± 0.00	1s*	$+1.03$
Dy II	1.14	$\cdots$			$\cdots$			-1.43 ± 0.07	2	$+0.83$

[†]Refers to synthesis of CH bands.

*The number of features synthesized for each element has been indicated.

We had two spectra of this object observed on March 2 and 3, 2011. The echelle grating setting being different on these two nights, the coverage in each echelle order was different, although some overlap existed. Hence we have conducted two independent abundance analyses for these two spectra. We found the same atmospheric parameters for these two epochs, which is not surprising given the long period of the object. The abundance analysis (Table 4) shows the star to be very metal-poor ([Fe/H] $= -2.3$) and unaffected by DG winnowing: the α-elements (Mg, Ca, Ti) have their expected $[\alpha/\text{Fe}]$ values and Sc is not underabundant. These abundances and the large radial velocity ($+265$ km s^{-1}) suggest halo membership. The C I lines are below the detection limit and the forbidden lines of O I indicate enhanced O abundance.

The most interesting feature was the detection of lines of several s-process elements present in both spectra. The metal-poor nature of this star was very helpful in detecting the features of these elements. In Figure 4 we have shown agreement between the synthesized and observed spectrum for several s-process elements. We do not find significant differences between the light and heavy s-process elements.

However, this object with RVC spectral characteristics however looks more or less like a twin of V453 Oph given the high radial velocities, low metallicity, C underabundance and mild s-process enrichment.
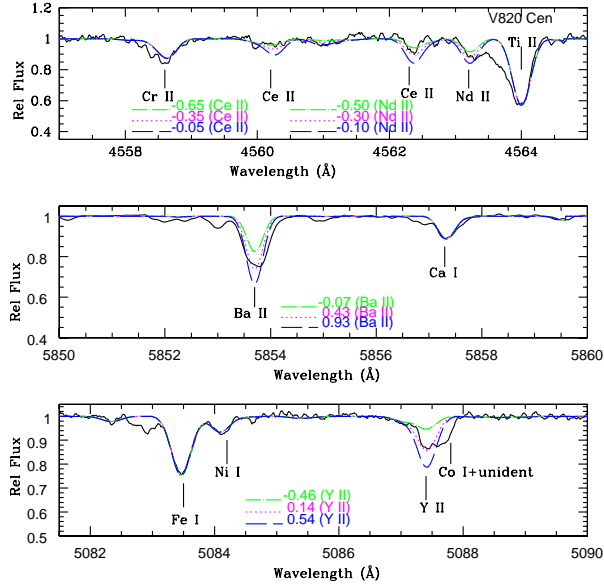
Fig. 4. The agreement between synthesized and observed spectrum for V820 Cen for selected regions containing the lines of s-process elements.

Fig. 5. Plot of [X/H] versus T_C for SU Gem.

5.1.3. IRAS 06108+2743

More popularly known as SU Gem, this star is a RVb variable with a pulsation period of 50 days and a long period of 690 days (Joy 1952). Preston et al. (1963) and Lloyd Evans (1985) assigned the spectroscopic type RVA. De Ruyter et al. (2005) constructed the SED for SU Gem and used an optically thin dust model to estimate the parameters of the dust shell and they suggested the possible dust distribution to be in a stable Keplerian disk. A detailed study of the IR spectra of SU Gem (Gielen et al. 2008) indicated the presence of amorphous and crystalline silicates, pointing towards an O-rich disk.

The chosen model (Table 2) gives the abundances listed in Table 5. Ionization equilibrium shown by $\Delta = [X_{II}/H] - [X_I/H]$ is -0.01, $+0.11$ and $+0.02$ for Fe, Ti and Cr respectively. The C abundance was derived from the synthesis of the C I line at 6587Å and the O abundance from the 6300 and 6363 Å forbidden lines. It is evident from Figure 5 that depletion of elements with the highest T_Cs like Ca, Sc, Ti, Al as well as the s-process elements point to mild DG winnowing.

5.1.4. IRAS 22223+5556

Also known as BT Lac, this star is a RV Tauri of the RVb class variable with a period of 40.5 days and a long period of 654 days (Tempesti 1955; Percy et al. 1997). The star was observed on the night of October 10, 2009 and has a V magnitude of 12.8
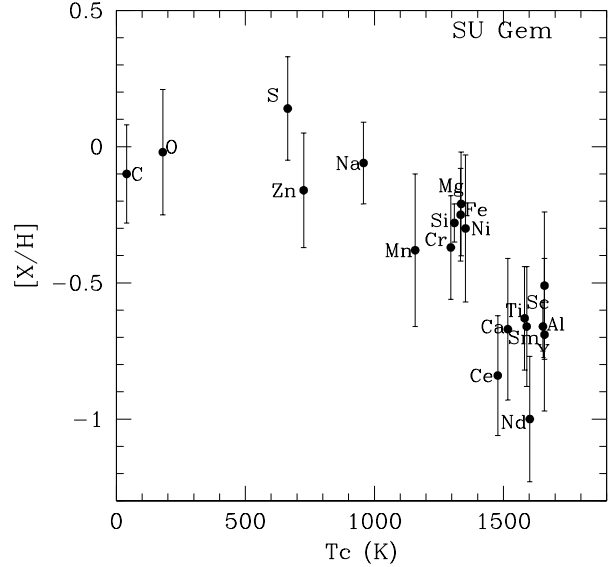
which is at the faint limit of the telescope. Hence the S/N ratio was only about $30-40$ even after co-adding four exposures each of 30 min duration. The number of usable lines was much smaller than what one would expect for this temperature and gravity, due to distorted profiles and suggestions of line doubling for several elements. Our analysis relies upon clean symmetrical lines. The metallicity of BT Lac is almost solar ([Fe/H]$=-0.2$). The O abundance has been determined from the forbidden line at 6300Å. The lines of C and S were distorted and appeared to be double and could not be used in our analysis. Mild DG winnowing is suggested by almost solar Zn abundance and underabundances of Ca, Sc, Ti and the s-process elements Y, Zr, Ce and Sm (see Table 5).

5.1.5. TX Per

This star was classified as a RVa variable in the GCVS (see also Percy & Coffey 2005). Zsoldos (1995) gave a period of 78 days. TX Per does not have IRAS colors. Planesas et al. (1991) showed that TX Per had no detected OH maser emission and had weak CO emission pointing to a deficiency of molecules in its envelope.

The abundance analysis (see Table 5) shows that the star is mildly metal-poor ([Fe/H] $= -0.58$). The C and N abundances could not be determined due to the low temperature of the star. The O abundance has been determined using the forbidden lines at 6300 and 6363 Å. The high condensation temperature elements ($T_C > 1500$ K) including α elements

Ca, Ti, and the s-process elements Zr and Ce, again with $T_C > 1500$ K, are slightly under-abundant, but no signature of DG winnowing is seen, as the low T_C element Zn is also underabundant.

5.1.6. *IRAS 19135+3937*

It is a relatively unexplored object; SIMBAD gives only IRAS fluxes and V magnitude. We list the star as RV-like based on its position in the IRAS two-color diagram (see Figure 1). A time-series monitoring of the high-resolution spectra for this star by Gorlova, van Winckel, & Jorissen (2012a) indicated radial-velocity variations of the order of $130-140$ days. Also, the Hα profile variations were found to correlate with the radial velocity phase, indicating the possibility of a faint companion surrounded by an accretion disk with an outflow.

Our spectrum is not ideal. All lines appear to have a red-shifted absorption component. We have measured a few reasonably clean lines. The lines of N and Si were heavily distorted indicating unresolved doubling and hence the abundances for these elements could not be determined. The star is metal poor with [Fe/H] of -1.0. The α elements Mg and S yield [α/Fe] of $+0.3$, which is expected at this metallicity. The other α elements Ca and Ti and the s-process elements have negative [X/H] values which defy simple explanation. As explained in Paper-1, the non-LTE correction for Ca I for this temperature and metallicity range could be in the $+0.1$ to 0.2 dex range. It is difficult to ascribe this to DG effect since Sc (an element with even higher T_C) is less deficient. Further, the expected enrichment of [Zn/Fe] in DG objects is not seen.

But IRAS 19135+3937, despite having suitable temperature, metallicity and being a possible member of a binary (Gorlova et al. 2012b), does not show a clear signature of DG winnowing, as is evident from abundances in Table 5. An overabundance of C I ([C/Fe]=$+0.8$ dex) is derived from the measurement of four reasonably clean (but asymmetric) lines. This star deserves further analysis with spectra at more stable phases.

5.2. *Extension of the existing analyses*

To further our understanding of these objects, we have undertaken a contemporary analysis using a new grid of model atmospheres, more accurate $\log gf$ and covering more elements.

5.2.1. *IRAS 01427+4633*

This was considered as a RV Tauri like object based upon its location in two color IRAS diagram and no photometry is available. Recently Gorlova et al. (2012b) conducted radial velocity monitoring of this object for nearly three years starting 2009, and also performed abundance analyses. Gorlova et al. (2012b) found this object to be a spectroscopic binary with an orbital period of 140.8 $\pm$0.2 days, eccentricity e of 0.083$\pm$0.002 and asini of 0.31 au.

The model parameters derived from our spectra are presented in Table 2. We estimate model atmospheric parameters ($T_{\rm eff}$, $\log g$, and ξ) of (6500, 0.5, 3.5) while Gorlova et al. (2012b) estimate (6250, 1.5, 4.0). Ionization equilibrium is satisfied since $\Delta = $ [X$_{\rm II}$/H] $-$ [X$_{\rm I}$/H] is -0.10, -0.06, $+0.01$ and $+0.01$ for Fe, Si, Ti and Cr respectively, as can be seen in Table 6.

The star is metal poor with [Fe/H] of -0.79 and is enriched in the α elements Mg, Si, Ca and Ti with an average [α/Fe] of $+0.34$. The low metallicity and the α abundances point towards thick disk membership. Enrichment of the light elements C, N and O suggests that the star has evolved beyond the red giant branch (RGB), but substantial exposure to thermal, pulses on the AGB is unlikely to have occurred, as the C/O ratio is around 0.5; the s-process elements are not overabundant.

The abundance analysis by Gorlova et al. (2012b) uses solar gf values normalised to solar abundances (Grevesse, Noels, & Sauval 1996) and model atmosphere by Kurucz (1992), while we use solar abundances from Asplund et al. (2005). We therefore chose to make the comparison using $\log \epsilon$ derived from the two studies. We find differences between Gorlova et al. (2012b) and our present work as follows: $+0.27$ for C, $+0.07$ for N, -0.11 for Mg, $+0.10$ for Si, -0.05 for S, -0.15 for Ca, -0.26 for Sc, -0.26 for Ti, $+0.06$ for Cr, $+0.04$ for Mn, -0.31 for Ni, -0.01 for Zn, -0.15 for Y and -0.13 for Ba. For the majority of elements the agreement is within ± 0.20 dex.

We did not find very convincing evidence for DG winnowing. Although [S/Fe] is $+0.37$, it could be attributed to the fact that it is an α element. In fact other α elements like Si and Ti also show similar enrichment, although [Ca/Fe] is relatively smaller. With [Zn/Fe] of -0.08 and positive [Sc/Fe], it is very unlikely that DG winnowing has affected this object. This star is similar to IRAS 07140-2321 studied in Paper-1, in the sense that despite favourable conditions such as warm temperature, presence of binary companion and circumstellar material the effect of DG winnowing is not seen, thereby highlighting our inadequate understanding of this effect.

5.2.2. *HD 52961*

HD 52961 is a high galactic latitude F type supergiant with a strong IR excess and it is a semi-regular (SRD) variable with a pulsation period of 70 days (Waelkens et al. 1991). The light curve exhibits the long-term RVb like phenomenon in the mean magnitude (seen in RV Tauri stars) thought to be caused by the variable circumstellar extinction during orbital motion (van Winckel et al. 1999). But the light curve does not exhibit alternate deep and shallow minima, typically seen in RV Tauri stars, and has been labeled as RV Tauri like object in Figure 1. Radial velocity monitoring was carried out by van Winckel et al. (1999) who report the star to be a spectroscopic binary with an orbital period of 1310 days.

Deroo et al. (2006) resolved the dusty disk of HD 52961 using *N*-band interferometry and found that the dust emission at 8 μm originates from a compact region of diameter 50 au. Gielen et al. (2009) analyzed a high resolution IR spectrum and found that it was dominated by spectral features from both amorphous and crystalline silicates. The high crystallinity fraction and large sized grains show that the dust grains are strongly processed and that the disk is long-lived. Even though the analysis of HD 52961 showing significant depletion of refractory elements in its photosphere was conducted (Waelkens et al. 1991; van Winckel 1995), an extensive abundance analysis with the most recent *gf* values was lacking.

Hence we have performed a detailed abundance analysis for HD 52961 (see Table 6) using our selection of *gf* values and Kurucz model atmospheres. We have compared our results with those of van Winckel (1995); agreement is within ±0.2 dex for elements in common. We were able to determine for the first time the abundance of Na, Mg, Si, Ca and Ti, as can be seen in Table 6. It has resulted in a better definition of the depletion curve. Figure 6 shows the plot of [X/H] versus T_C for HD 52961, a classic case of DG winnowing.

5.2.3. *V453 Oph*

This is a RV Tauri variable of spectroscopic type RVC and photometric type RVa. A photometric period of 80 days was obtained by Pollard et al. (1996). The star does not have an IR excess (Deroo et al. 2005).

Our spectrum gives model parameters (T_{eff} = 5750 K, log g =1.50, and ξ_t = 3.7 km s^{-1}) similar to those derived by Deroo et al. (2005) (T_{eff} = 6250 K, log g = 1.50, and ξ_t = 3.0 km s^{-1}). The star is variable, so exact agreement for the atmospheric
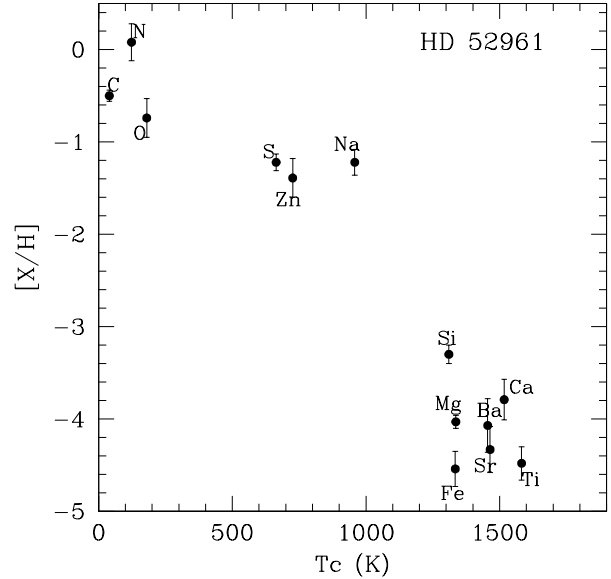

Fig. 6. Plot of [X/H] versus T_C for HD 52961.

parameters is not expected. It would appear that we observed the star at a slightly cooler phase than Deroo et al. (2005). The abundances are in good agreement. We find δ [X/Fe] (present work − Deroo et al. 2005) of +0.13 for C, −0.12 for O, +0.06 for Mg, +0.15 for Al, +0.18 for Si, −0.04 for Ca, −0.12 for Sc, +0.04 for Ti, −0.10 for Cr, +0.30 for Mn, −0.13 for Ni, +0.23 for Zn, +0.06 for Y, +0.07 for Zr, −0.06 for Ba, +0.23 for La, +0.19 for Ce, −0.02 for Nd, +0.32 for Eu and +0.15 for Dy. We could determine the additional elements Na and the s-process element Gd for this star. But the N abundance could not be determined, as our spectrum was obtained at a cooler phase than that of Deroo et al. (2005).

The metal abundances and the high radial velocity (-126 kms^{-1}) suggest that V453 Oph is a member of the galactic halo. There is no evidence that DG winnowing has affected the star. An interesting feature is the clear s-process enrichment reported first by Deroo et al. (2005). The mean enrichment [s/Fe] is about +0.6 with possibly a larger enrichment for the heavy (Ba-Gd) than for the light (Y, Zr) elements as can be seen in Table 6. This enrichment is presumably the result of third dredge-up (TDU) in the AGB progenitor but the lack of a C-enrichment, also reported by Deroo et al. (2005), is puzzling. (Our C abundance is obtained from CH lines at 4300−4320 Å. Deroo et al.'s 2005 C abundance was obtained from the synthesis of C lines around 9070 Å).

TABLE 7

A COMPILATION OF RV TAURI AND RV TAURI LIKE VARIABLES
SHOWING DG WINNOWING AND FIP EFFECT

Star	T_{eff}	V[a]	S[b]	[S/H]	[Zn/H]	[Sc/H]	[Ca/H]	[Ti/H]	[Fe/H]	[Fe/H]$_{\mathrm{o}}$[c]	DI[d]	P[e]	L[f]	Bin[g]	Ref
						Depleted (DG) RV Tauri Stars									
HP Lyr	6300	$\cdots$	B	+0.0	−0.3	−2.8	−1.9	−2.9	−0.9	−0.2	2.8	141	3.8	Y	2
DY Ori	6000	a	B	+0.2	−0.2	−2.9	−2.2	−2.3	−2.2	+0.0	2.7	60	3.2	N	2
IW Car	6700	b	B	+0.4	−0.0	−2.1	−1.9	$\cdots$	−1.0	+0.2	2.4	68	3.3	N	9
AD Aql	6300	a	B	−0.0	−0.1	−1.8	−2.2	−2.6	−2.1	−0.1	2.2	65	3.3	N	6
AR Pup	6000	b	B	+0.4	$\cdots$	−2.2	−1.4	$\cdots$	−0.9	+0.4?[i]	2.2	75	3.4	Y	5
17233-4330*	6250	b	B	+0.1	−0.2	−1.6	−1.4	−1.6	−1.0	−0.1	1.7	$\cdots$	$\cdots$	N	8
UY CMa	5500	a	B	−0.3	−0.6	−2.2	−1.6	−2.4	−1.3	−0.5	1.7	114	3.7	N	2
CT Ori	5500	a	B	−0.5	−0.5	−2.5	−1.8	−2.5	−1.8	−0.5	1.7	136	3.8	N	4
SX Cen	6500	b	B	−0.1	−0.5	−1.9	−1.5	−1.9	−1.1	−0.3	1.6	33	2.8	Y	7
R Sge	5750	b	A	+0.4	−0.2	−1.5	−0.9	−1.3	−0.5	+0.1	1.6	71	3.4	N	5
UZ Oph	5000	a	A	−0.4	−0.7	−1.3	−1.1	−1.0	−0.7	−0.8	1.5	87	3.5	N	2
RX Cap	5800	$\cdots$	A	−0.6	−0.6	−1.2	−0.8	−0.6	−0.8	−0.6	1.4	68	3.3	N	2
UY Ara	5500	a	B	+0.0	−0.3	−1.7	−1.1	$\cdots$	−1.0	−0.2	1.4	58	3.2	N	1
AZ Sgr	4750	a	A	−0.3	$\cdots$	−1.8	−1.8	−1.6	−1.6	−0.3?[i]	1.4	114	3.8	N	2
BZ Sct	6250	$\cdots$	B	+0.2	+0.0	−1.1	−0.9	−1.2	−0.8	+0.1	1.3	$\cdots$	$\cdots$	N	2
EP Lyr	5750	b	B	−0.6	−0.7	−2.1	−1.8	−2.0	−1.8	−0.9	1.3	83	3.5	Y	5
SS Gem	5500	a	B	−0.4	+0.0	−1.9	−1.0	−2.0	−0.8	−0.2	1.2	89	3.5	N	4
16230-3410*	6250	$\cdots$	A	−0.4	−0.4	−2.3	−0.7	−1.4	−0.7	−0.4	1.1	$\cdots$	$\cdots$	N	8
LR Sco	6250	a	B	+0.0	+0.2	−1.1	−0.2	−0.6	−0.0	+0.1	1.1	104	3.6	Y	2
RU Cen	6000	a	B	−0.7	−1.0	−1.9	−1.9	−1.9	−1.9	−1.1	1.1	65	3.3	Y	7
AC Her	6000	a	B	−0.4	−0.9	−1.7	−1.5	−1.6	−1.4	−0.9	1.1	75	3.4	Y	6
TT Oph	4800	a	A	+0.0	−0.7	−1.1	−1.1	−0.8	−0.8	−0.8	1.0	61	3.3	N	1
V Vul	4500	a	A	+0.6	−0.3	−0.7	−0.5	−0.2	−0.4	+0.1	1.0	76	3.6	N	2
						Mildly Depleted (MDG) RV Tauri Stars									
AI Sco	5300	b	A	−0.1	−0.6	−0.9	−0.6	−0.9	−0.7	−0.3	0.8	71	3.4	N	2
TX Oph	5000	$\cdots$	A	−0.6	−1.2	−1.8	−1.4	−1.2	−1.2	−1.1	0.8	135	3.8	N	2
SU Gem	5250	b	A	+0.1	−0.1	−0.5	−0.7	−0.6	−0.2	+0.0	0.7	50	3.2	N	3
U Mon	5000	b	A	−0.1	−0.7	−0.9	−0.9	−0.7	−0.8	−0.6	0.7	91	3.6	Y	1
R Sct	4500	a	A	$\cdots$	−0.2	−1.4	$\cdots$	−0.4	−0.4	−0.2	0.7	147	4.0	N	1
17038-4815*	4750	a	A	$\cdots$	−1.2	−2.0	−1.4	−1.9	−1.5	−1.2	0.6	$\cdots$	$\cdots$	Y	8
BT Lac	5000	b	A	$\cdots$	−0.1	−0.5	−0.6	−0.6	−0.2	−0.1	0.5	41	3.0	N	3
DY Aql	4250	$\cdots$	A	$\cdots$	$\cdots$	−2.1	−1.2	$\cdots$	−1.0	$\cdots$	$\cdots$	131	4.0	N	4
						Depleted (DG) RV Tauri like Stars[h]									
AF Crt	5750	RV like	$\cdots$	−0.5	−0.9	−4.2	−2.7	$\cdots$	−2.7	−0.9	3.9	32	$\cdots$	Y	13
HD 52961	6000	RV like	$\cdots$	−0.9	−1.3	$\cdots$	$\cdots$	$\cdots$	−4.5	−1.3	3.8	71	$\cdots$	Y	3
						Depleted (DG) RV Tauri Stars in the LMC									
82.8405.15[†]	6000	$\cdots$	$\cdots$	−0.3	−0.3	−3.1	−2.1	−2.8	−2.5	−0.3	2.3	93	3.5	N	11
79.5501.13[†]	5750	$\cdots$	$\cdots$	−0.6	−0.6	−3.0	−1.7	−2.8	−1.8	−0.6	1.9	97	3.6	N	12
81.8520.15[†]	6250	$\cdots$	$\cdots$	$\cdots$	−1.4	−1.9	−1.5	−1.9	−1.6	−1.4	0.4	84	3.5	N	12
81.9728.14[†]	5750	$\cdots$	$\cdots$	$\cdots$	−1.2	−2.0	−1.1	−1.8	−1.1	−1.2	0.4	94	3.6	N	12
						FIP affected RV Tauri Stars									
CE Vir	4250	$\cdots$	A	$\cdots$	−0.7	−2.5	−1.6	−1.0	−1.0	−0.7	$\cdots$	67	3.5	N	10
EQ Cas	5300	a	B	−0.3	−0.3	−3.1	−2.0	−1.3	−0.8	−0.3	$\cdots$	58	3.3	N	2

[†]Refers to the RV Tauri stars in the LMC discovered by Alcock et al. (1998) through the MACHO (Massive Compact Halo Object) project. *Stands for IRAS name. [a]Variability Type deduced from the behaviour of the light curves. a and b represent the RV Tauri photometric type which has been explained in the introduction part of this paper. [b]Spectroscopic Type: A, B and C refer to the Preston's spectroscopic type for RV Tauri stars explained in detail in the introduction part of this paper. [c][Fe/H]$_{\mathrm{o}}$ refers to the initial metallicity and is calculated by taking the average of [S/H] and [Zn/H]. [d]DI refers to Depletion Index given by DI = [S/H]-([Ca/H]+[Sc/H]+[Ti/H])/3. In the absence of other elements DI is calculated from S and Fe. [e]P refers to Pulsational Period in Days. [f]L refers to $\log(L/L_{\odot})$ and are the luminosities of the stars calculated from the P-L relation given by Alcock et al. (1998). [g]Bin refers to binarity. The direct evidence for binarity comes from radial velocity monitoring (Y) while the other stars (N) do not have binary detections as of now. [h]The RV Tauri like stars do not have published light curves and photometry. These have RV Tauri like IR colors in the two-color diagram and have been considered in this study. [i]Uncertain [Fe/H]$_{\mathrm{o}}$ due to unavailability of [Zn/H]. References: 1. Giridhar, Lambert, & Gonzalez 2000; 2. Giridhar et al. 2005; 3. Present Work; 4. Gonzalez, Lambert, & Giridhar 1997a; 5. Gonzalez, Lambert, & Giridhar 1997b; 6. Giridhar, Lambert, & Gonzalez 1998; 7. Maas, van Winckel, & Waelkens 2002; 8. Maas, van Winckel, & Lloyd Evans 2005; 9. Giridhar, Rao, & Lambert 1994; 10. Rao & Reddy 2005; 11. Reyniers & van Winckel 2007; 12. Gielen et al. 2009; 13. van Winckel et al. 2012.

TABLE 8

A COMPILATION OF RV TAURI AND RV TAURI LIKE VARIABLES SHOWING
S-PROCESS ENRICHMENT AND NORMAL COMPOSITIONS

Star	$T_{\rm eff}$	V[a]	S[b]	[S/H]	[Si/H]	[Ca/H]	[Fe/H]	[s/Fe][c]	P[d]	L[e]	Bin[f]	Ref
				s-process Enriched RV Tauri Stars								
V453 Oph	5750	a	C	$\cdots$	−1.7	−2.1	−2.2	+0.7	81	3.5	N	3
V820 Cen	4750	a	C	$\cdots$	$\cdots$	−1.7	−1.9	+0.4	150	3.9	N	3
				s-process Enriched RV Tauri Like Star[g]								
06165+3158*	4250	RV like	$\cdots$	$\cdots$	−0.9	−1.2	−0.9	+0.4	$\cdots$	$\cdots$	N	3
				s-process Enriched RV Tauri Star in the LMC								
47.2496.8†	4900	$\cdots$	$\cdots$	$\cdots$	$\cdots$	−1.9	−1.5	+1.8	113	3.8	N	7
				s-process Enriched RV Tauri like Star in the LMC								
J050632.10-714229.8	6750	$\cdots$	$\cdots$	−1.2	−0.6	−1.4	−1.2	+1.2	49	3.7	N	8
				Normal Composition RV Tauri Stars								
BZ Pyx	6500	b	B	−0.7	−0.6	−0.5	−0.7	+0.2	$\cdots$	$\cdots$	Y	5
DS Aqr	6500	a	C	−0.8	−0.8	−1.0	−1.1	−0.1	77	3.4	N	1
EN TrA	6000	$\cdots$	B	−0.6	−0.6	−1.0	−0.8	$\cdots$	37	2.9	Y	6
BT Lib	5800	$\cdots$	C	−0.8	−0.7	−0.9	−1.2	+0.5?[g]	75	3.4	N	1
09538-7622*	5500	b	A	−0.3	+0.0	−0.6	−0.6	−0.5	$\cdots$	$\cdots$	N	5
AR Sgr	5300	a	A	−0.8	−0.8	−1.4	−1.5	−0.1	88	3.5	N	2
V360 Cyg	5250	a	C	−0.9	−0.9	−1.3	−1.4	+0.0	70	3.4	N	4
DF Cyg	4800	a	A	$\cdots$	+0.1	−0.2	−0.0	−0.7	50	3.2	N	2
TW Cam	4800	a	A	+0.0	−0.1	−0.7	−0.5	+0.1	87	3.6	N	1
RV Tau	4500	b	A	$\cdots$	−0.3	−0.5	−0.4	−0.4	79	3.6	N	1
TX Per	4250	a	A	$\cdots$	−0.2	−1.1	−0.6	−0.8	78	3.6	N	3
				Normal Composition RV Tauri Like Stars[g]								
01427+4633*	6500	RV like	$\cdots$	−0.4	−0.4	−0.7	−0.7	−0.1	$\cdots$	$\cdots$	Y	3
19135+3937*	6000	RV like	$\cdots$	−0.7	$\cdots$	−1.3	−1.0	−0.4	$\cdots$	$\cdots$	Y	3

†Refers to the RV Tauri stars in the LMC discovered by Alcock et al. (1998) through the MACHO (Massive Compact Halo Object) project. *Stands for IRAS name. [a]Variability Type deduced from the behaviour of the light curves. a and b represent the RV Tauri photometric type which has been explained in the introduction part of this paper. [b]Spectroscopic Type: A, B and C refer to the Preston's spectroscopic type for RV Tauri stars explained in detail in the introduction part of this paper. [c][s/Fe] corresponds to the average of all the s-process elements. [d]P refers to Pulsational Period in Days. [e]L refers to $\log(L/L_{\odot})$ and are the luminosities of the stars calculated from the P-L relation given by Alcock et al. (1998). [f]Bin refers to binarity. The direct evidence for binarity comes from radial velocity monitoring (Y) while the other stars (N) do not have binary detections as of now. [g]The RV Tauri like stars do not have published light curves and photometry. These have RV Tauri like IR colors in the two-color diagram and have been considered in this study. [h]Uncertain abundance as it is based on single line measurement of Ba II. References: 1. Giridhar, Lambert, & Gonzalez 2000; 2. Giridhar et al. 2005; 3. Present Work; 4. Giridhar, Lambert, & Gonzalez 1998; 5. Maas, van Winckel, & Lloyd Evans 2005; 6. van Winckel 1997; 7. Reyniers et al. 2007; 8. van Aarle et al. 2013.

6. DISCUSSION

6.1. *Chemical compositions of RV Tauri stars*

From the compilation of the existing data on the chemical compositions of RV Tauri and RV Tauri like objects presented in Tables 7 and 8, it can be seen that they can be divided into certain characteristic groups. A significant fraction are affected by DG winnowing, another subgroup shows normal composition of evolved red giants. Although s-process enhancement is not commonly seen for galactic RV Tauri stars, a few RVCs (two) show mild s-process enhancement. On the other hand, in the LMC, one RV Tauri star showing significant s-process enhancement has been detected. A couple of galactic RV Tauri stars showing abundance peculiarities correlated with their FIP have also been reported. The stars affected by the DG and the FIP effect are presented in Table 7, while Table 8 lists stars with s-process enhancement and those showing normal composition.

The definitions of DI and other parameters listed in Tables 7 and 8 are given in their footnotes, respectively. The stars in each category are arranged in order of decreasing temperatures. Stars with and without binary detections are marked as Y and N in Tables 7 and 8. We choose to list only binary detections confirmed via direct evidence like radial velocity monitoring. This has resulted in a smaller fraction of binarity compared to other workers (De Ruyter et al. 2006; Gielen et al. 2011) where the detections are based on indirect evidence like the presence of broad near IR excess (hot dust closer to the star indicating the possible presence of a dusty circumbinary disk) in their SEDs. This number may change when more detections are reported.

6.1.1. *RV Tauri objects showing depletion of refractory elements*

The main signature of DG winnowing is an observed dependence of depletion of condensable elements on the predicted T_C. Since Fe is also found to be depleted by this process, it cannot be the true indicator of intrinsic metallicity; hence, Zn and S, which are least affected by this process (due to their low T_Cs), would serve as metallicity indicators. We have calculated the intrinsic metallicity: $[Fe/H]_o$ by taking the average of $[S/H]$ and $[Zn/H]$. For two stars values for $[Zn/H]$ were not available; hence, we have used only $[S/H]$. The S being α element, the intrinsic metallicity could be overestimated for thick disk and halo objects; hence, for stars with $[Zn/H]$ lower than -0.7 dex, a correction of 0.3 dex for S (see e.g., Maas, Giridhar, & Lambert 2007) and 0.1 dex for Zn (see Reddy, Lambert, & Allende Prieto 2006) has been applied to the calculation of $[Fe/H]_o$ for these objects. We consider the star to be well depleted when $[Zn/Fe]$ is positive, $[Sc/Fe]$ negative, DI ≥ 1.0 and are denoted as DG in Table 7. Some stars have an incomplete signature of DG winnowing in the sense that $[Sc/Fe]$ is negative while $[Zn/Fe]$ is normal and DIs < 1.0. Such objects are considered as stars for which the DG winnowing is mild and are denoted as MDG in Table 7.

Similar to the post-AGBs[3], the boundary conditions for discernible DG, i.e., minimum effective temperature and intrinsic metallicity (as discussed

in Paper-1) are also observed for the RV Tauri stars. These limits are 4500 K in temperature and $[Fe/H]_o \sim -1.0$ for intrinsic metallicity, not very different from those found for post-AGBs (Rao et al. 2012). As explained in Giridhar et al. (2000), at cooler temperatures a deeper convective envelope dilutes the accreted gas weakening the abundance anomalies. Below the above mentioned metallicity limit the lower dust mass fraction results in the inability of the radiation pressure on dust grains to cause DG separation.

The variation in DG index suggests a dependence on several other factors such as (i) the composition of the gas and dust in the reservoir from which the star draws gas and the temperature distribution within the reservoir (ii) the rate and degree of mixing of the accreted material with the atmosphere/envelope of the star.

There is a growing consensus that the DG winnowing is most effective in RV Tauri variables that belong to a binary system with a circumbinary dusty disk providing the reservoir from which gas is accreted by the RV Tauri star (Maas et al. 2005; van Winckel 2007). For the DG and MDG galactic RV Tauri and RV Tauri like stars in Table 7, only 11 out of 33 (33%) objects have confirmed binary detections (via radial velocity monitoring). The orbital parameters are known accurately only for a handful of these objects, as the detection of binarity is rendered challenging due to the presence of stellar pulsations; passage of shock waves during certain phases causes line deformation/splitting. Also the radial velocity measurements need to be carried out over several pulsation cycles due to their long periods. This requires very long observing times. High spatial resolution interferometry and radial velocity monitoring are required to improve our understanding of these objects.

In the present work we have detected mild DG winnowing effects in the additional RV Tauri objects: SU Gem and BT Lac; the mildness of DG effects may be ascribed to their low effective temperatures. However, these stars do not have binary detections and hence radial velocity monitoring has to be carried out to confirm binarity.

6.1.2. *RV Tauris with FIP effect*

While one generally encounters a normal composition, depletion of refractory elements, (not so common) mild s-process enrichment among RV Tauri stars, a couple (CE Vir and EQ Cas) exhibited a very peculiar abundance distribution marked by Na deficiency (see Table 7). Rao & Reddy (2005) showed

---

[3]Here we refer to post-AGBs as the ones whose light curves exhibit small amplitude (0.05−0.5 magnitude) irregular pulsations and do not show the typical alternating pattern seen in RV Tauri stars which exhibit large amplitude (0.5−1.5 magnitude) pulsations (Kiss et al. 2007). From the positions of RV Tauris and a limited sample of post-AGBs with known parallaxes in the H-R diagram, it appears that post-AGBs might be systematically more evolved than RV Tauris.

that the observed abundances were related to the their FIP (hence the name FIP effect). These authors proposed that the effect resulted from systematic removal of singly ionized species in the photospheres of these stars under the influence of outflowing magnetized columns of gas. The atoms with large FIP were in neutral state at these temperatures. Hence, they were unaffected, while those with lower FIP were ionized and hence were moved away along with the outflow, and therefore systematically removed. We are not aware of any further addition to this group.

6.1.3. *RV Tauris with s-process enrichment*

The only known galactic RV Tauri object showing s-process enrichment had been V453 Oph − an RVC object of long period (80 days). In this work, we report a mild s-process enhancement in yet another long period (150 days) RVC object V820 Cen. Both these objects exhibit large radial velocities, are metal-poor (expected for RVC), have no detected IR excess and also show the α enhancement seen in metal-poor stars.

Both V820 Cen and V453 Oph could possibly be single stars; there is neither evidence through radial velocity study nor indirect evidence through the detection of warm circumstellar matter near the star as they have no detected IR excess. A long term radial velocity monitoring over several pulsation cycles would be required to resolve the issue. Since only 1% of post-AGB stars are expected to show extrinsic s-process enrichment (through mass-transfer caused by an evolved companion) and no RV Tauris with evolved companions have been detected so far (van Aarle et al. 2013; Deroo et al. 2005), it is more likely that these RVC objects are genuinely thermally pulsing (TP)-AGB stars.

It appears that RVC objects are promising candidates to analyse s-processing in RV Tauris. The models of AGB evolution predict that stars in the mass range 1.8 to 4.0 $M_\odot$ would experience TDU and show s-process enhancement (Herwig 2005) but at lower metallicity TDU can take place even at lower masses (see Tables 2 and 3 of Karakas, Lattanzio, & Pols 2002). These authors have also pointed out the influence of mass-loss on the AGB evolution in further lowering this mass limit.

Hence it is possible that the metal-poor environment of RVC might allow thermal pulses and efficient TDU even at the RV Tauri like lower mass (0.8 to 1.5 $M_\odot$) see Deroo et al. (2005) and Reyniers et al. (2007) for mass estimates. This suggestion is not unreasonable since the s-process enriched RV Tauri

star detected in the metal-poor environment of the LMC: MACHO 47.2496.8 (studied by Reyniers et al. 2007) exhibits clear indications of s-process enhancement.

However there is a major difference; the LMC RV Tauri has C/O greater than 1 and [s/Fe] is quite large +1.2 for lighter and +2.1 for heavier s-process elements. Galactic RV Tauris exhibit very mild s-processing without carbon enrichment (see Table 8). Hence a scenario based upon nucleosynthesis could be an oversimplification.

V453 Oph ([Fe/H]=−2.1) and V820 Cen ([Fe/H]=−2.2) are more metal-poor than the RVC stars studied so far. One wonders if there is a metallicity limit below which RVC might show s-processing? We have reservations about considering IRAS 06165+3158 in this group for several reasons. It is a RV Tauri like object with no photometry; although it is metal-poor with moderate s-process enhancement, the α enrichment is not seen nor does it show high radial velocity expected of RVC objects.

6.1.4. *RV Tauris showing normal composition*

About one fourth of the galactic RV Tauri (with and without binary detections) and RV Tauri like stars exhibit normal composition i.e. they exhibit the signature of ISM for heavy elements while light elements may show the effect of CN processing (see Table 8). For significantly metal-poor stars the expected α enrichment is observed. Binarity is not very common, although a small fraction have binary detections. Their normal compositions is understandable as most of them belong to the RVA and C spectroscopic classes; hence, they do not meet the boundary conditions for DG effects. However, IRAS 19135+3937 and IRAS 01427+4633 (see Table 8) pose a challenge. Despite these objects having favorable conditions for depletion, like the presence of strong IR excess, conducive effective temperatures and binarity, they do not show the effects of DG winnowing!

The absence of an observed DG effect in these objects might be due to two reasons. Firstly, these objects are all short period binaries having orbital periods and $a\sin i$ in the range of 127−141 days and 0.2−0.3 au respectively. (The orbital period range and $a\sin i$ for depleted (DG) objects are usually in the range of 300−1300 days and 0.4−1.6 au). An optimised orbital period range seems to be an additional condition for DG to operate.

Secondly for these objects Gorlova et al. (2012a,b) report a strong P-Cygni Hα profile with blue shifted absorption components indicating large

expansion velocities and splitting of strong metal lines, which is attributed to the ongoing mass-loss induced by the companion. This may be responsible for the absence of depletions observed in these stars. But there is no ready explanation for BZ Pyx a binary with an IR excess and orbital period of 371 days. We have not yet identified all operators/necessary conditions controlling the DG effect.

7. SUMMARY AND CONCLUSIONS

In this paper we have made a detailed abundance analysis using high resolution spectra of relatively unexplored RV Tauri stars and stars having RV Tauri like colors from its position in the IRAS two-color diagram. A more extensive abundance analysis for the stars V453 Oph and HD 52961 was also undertaken. With the study of additional elements, a better defined depletion curve for HD 52961 is obtained. Our findings are summarized below:

• A mild suggestion of DG winnowing is seen in the RV Tauri objects SU Gem and BT Lac. No abundance peculiarities are observed in IRAS 01427+4633 and IRAS 19135+3937 despite their binarity and the existence of circumstellar material surrounding them.

• The detection of small but significant s-processing in yet another RVC star: V820 Cen is very important as it makes them possible candidates to study nucleosynthesis near the low mass end of the AGB stars. However, it is difficult to account for the lack of carbon enrichment in these objects. Mild s-processing is also detected in the star IRAS 06165+3158, an object with RV Tauri like IRAS colors. Further photometric and spectroscopic monitoring is required to understand its variable nature.

Optical-Infrared High-Resolution campaigns of selected RV Tauri stars over their pulsation periods may help in understanding various abundance patterns observed in these fascinating objects. Such a study may also unravel the possible role of pulsations/stellar wind in sustaining depletion. One cannot exaggerate the importance of photometric and radial velocity monitoring towards the increased detection of binary companions.

Continued studies of unexplored galactic and extragalactic RV Tauri stars could be very rewarding as exemplified by the detection of a few depleted and one s-process enriched RV Tauri stars in the LMC.

REFERENCES

Alcock, C., et al. 1998, AJ, 115, 1921

Asplund, M., Grevesse, N., & Sauval, A. J. 2005, in ASP Conf. Ser. 336, Cosmic Abundances as Records of Stellar Evolution and Nucleosynthesis, ed. Thomas G. Barnes III & Frank N. Bash (San Francisco: ASP), 25

Bond, H. E. 1991, in IAU Symp. 145, Evolution of Stars: the Photospheric Abundance Connection, ed. G. Michaud & A. Tutukov (Dordrecht: Kluwer), 341

Deroo, P., Reyniers, M., van Winckel, H., Goriely, S., & Siess, L. 2005, A&A, 438, 987

Deroo, P., et al. 2006, A&A, 450, 181

De Ruyter, S., van Winckel, H., Dominik, C., Waters, L. B. F. M., & Dejonghe, H. 2005, A&A, 435, 161

De Ruyter, S., van Winckel, H., Maas, T., Lloyd Evans, T., Waters, L. B. F. M., & Dejonghe, H. 2006, A&A, 448, 641

Eggen, O. J. 1986, AJ, 91, 890

Gielen, C., van Winckel, H., Matsuura, M., Min, M., Deroo, P., Waters, L. B. F. M., & Dominik, C. 2009, A&A, 503, 843

Gielen, C., van Winckel, H., Min, M., Waters, L. B. F. M., & Lloyd Evans, T. 2008, A&A, 490, 725

Gielen, C., et al. 2011, in ASP Conf. Ser. 445, Why Galaxies Care About AGB Stars II: Shining Examples and Common Inhabitants, ed. F. Kerschbaum, T. Lebzelter, & R. F. Wing (San Francisco: ASP), 281

Giridhar, S., Lambert, D. L., & Gonzalez, G. 1998, ApJ, 509, 366

_____. 2000, ApJ, 531, 521

Giridhar, S., Lambert, D. L., Reddy, B. E., Gonzalez, G., & Yong, D. 2005, ApJ, 627, 432

Giridhar, S., Rao, N. K., & Lambert, D. L. 1994, ApJ, 437, 476

Gonzalez, G., Lambert, D. L., & Giridhar, S. 1997a, ApJ, 481, 452

_____. 1997b, ApJ, 479, 427

Gorlova, N., van Winckel, H., & Jorissen, A. 2012a, Baltic Astron., 21, 165

Gorlova, N., et al. 2012b, A&A, 542, A27

Grevesse, N., Noels, A., & Sauval, A. J. 1996, in ASP Conf. Ser. 99, Cosmic Abundances, ed. S. S. Holt & G. Sonneborn (San Francisco: ASP), 117

Herwig, F. 2005, ARA&A, 43, 435

Joy, A. H. 1952, ApJ, 115, 25

Jura, M. 1986, ApJ, 309, 732

Karakas, A. I., Lattanzio, J. C., & Pols, O. R. 2002, PASA, 19, 515

Kiss, L. L., Derekas, A., Szabó, G. M., Bedding, T. R., & Szabados, L. 2007, MNRAS, 375, 1338

Kukarkin, B. V., Parenago, P. P., & Kholopov, P. N. 1958, General Catalogue of Variable Stars (2nd ed.; Moscow: Academy of Sciences USSRR)

Kurucz, R. L. 1992, in IAU Symp. 149, The Stellar Populations of Galaxies, ed. B. Barbuy & A. Renzini (Dordrecht: Kluwer), 225

Lewis, B. M., Eder, J., & Terzian, Y. 1990, ApJ, 362, 634

Lloyd Evans, T. 1985, MNRAS, 217, 493

_____. 1999, in IAU Symp. 191, Asymptotic Giant Branch Stars, ed. T. Le Bertre, A. Lebre, & C. Waelkens (San Francisco: ASP), 453

Maas, T., Giridhar, S., & Lambert, D. L. 2007, ApJ, 666, 378

Maas, T., van Winckel, H., & Lloyd Evans, T. 2005, A&A, 429, 297

Maas, T., van Winckel, H., & Waelkens, C. 2002, A&A, 386, 504

Mathis, J. S., & Lamers, H. J. G. L. M. 1992, A&A, 259, L39

McWilliam, A. 1998, AJ, 115, 1640.

Miroshnichenko, A. S., et al. 2007, ApJ, 671, 828

Mucciarelli, A., Caffau, E., Freytag, B, Ludwig, H.-G., & Bonifacio, P. 2008, A&A, 484, 841

Percy, J. R., Bezuhly, M., Milanowski, M., & Zsoldos, E. 1997, PASP, 109, 264

Percy, J. R., & Coffey, J. 2005, J. Am. Ass. Variable Star Obs., 33, 193

Planesas, P., Bujarrabal, V., Le Squeren, A. M., & Mirabel, I. F. 1991, A&A, 251, 133

Pollard, K. R., Cottrell, P. L., Kilmartin, P. M., & Gilmore, A. C. 1996, MNRAS, 279, 949

Preston, G. W., Krzeminski, W., Smak, J., & Williams, J. A. 1963, ApJ, 137, 401

Prochaska, J. X., & McWilliam, A. 2000, ApJ, 537, L57

Rao, N. K., & Reddy, B. E. 2005, MNRAS, 357, 235

Rao, N. K., Sriram, S., Jayakumar, K., & Gabriel, F. 2005, J. Astrophys. Astron., 26, 331

Raveendran, A. V. 1989, MNRAS, 238, 945

Reddy, B. E., Lambert, D. L., & Allende Prieto, C. 2006, MNRAS, 367, 1329

Reyniers, M., Abia, C., van Winckel, H., Lloyd Evans, T., Decin, L., Eriksson, K., & Pollard, K. R. 2007, A&A, 461, 641

Reyniers, M., & van Winckel, H. 2007, A&A, 463, L1

Rao, S. S., Giridhar, S., & Lambert, D. L. 2012, MNRAS, 419, 1254 (Paper-1)

Tempesti, P. 1955, Mem. Soc. Astron. Italiana, 26, 125

Tull, R. G., MacQueen, P. J., Sneden, C., & Lambert, D. L. 1995, PASP, 107, 251

van Aarle, E., van Winckel, H., De Smedt, K., Kamath, D., & Wood, P. R. 2013, A&A, 554, A106

van Winckel, H. 1995, PhD Thesis, K. U. Leuven, Belgium

van Winckel, H. 1997, A&A, 319, 561

van Winckel, H. 2003, ARA&A, 41, 391

van Winckel, H. 2007, Baltic Astron., 16, 112

van Winckel, H., Hrivnak, B. J., Gorlova, N., Gielen, C., & Lu, W. 2012, A&A, 542, A53

van Winckel, H., Mathis, J. S., & Waelkens, C. 1992, Nature, 356, 500

van Winckel, H., Waelkens, C., Fernie, J. D., & Waters, L. B. F. M. 1999, A&A, 343, 202

van Winckel, H., Waelkens, C., Waters, L., Molster, F., Udry, S., & Bakker, E. 1998, A&A, 336, L17

Venn, K. A., & Lambert, D. L. 1990, ApJ, 363, 234

Waelkens, C., van Winckel, H., Bogaert, E., & Trams, N. R. 1991, A&A, 251, 495

Waelkens, C., & Waters, L. B. F M. 1993, in ASP Conf. Ser. 45, Luminous High-Latitude Supergiants, ed. D. D. Sasselov (San Francisco: ASP), 219

Wallerstein, G. 2002, PASP, 114, 689

Waters, L. B. F. M., Trams, N. R., & Waelkens, C. 1992, A&A, 262, L37

Zsoldos, E. 1995, J. British Astron. Assoc., 105, 238

S. Sumangala Rao and Sunetra Giridhar: Indian Institute of Astrophysics, Bangalore 560034, India (sumangala, sunetra@iiap.res.in).